Approximate Stability Analysis for Drystacked Structures

Yifang Liu[1], Maira Saboia[1], Vivek Thangavelu[1], and Nils Napp[1]

***Abstract*— We introduce a fast approximate stability analysis into an automated dry stacking procedure. Evaluating structural stability is essential for any type of construction, but especially challenging in techniques where building elements remain distinct and do not use fasteners or adhesives. Due to the irregular shape of construction materials, autonomous agents have restricted knowledge of contact geometry, which makes existing analysis tools difficult to deploy. In this paper, a geometric safety factor called *kern* is used to estimate how much the contact interface can shrink and the structure still be feasible, where feasibility can be checked efficiently using linear programming. We validate the stability measure by comparing the proposed methods with a fully simulated shaking test in 2D. We also improve existing heuristics-based planning by adding the proposed measure into the assembly process.**

I. Introduction

Robots that can autonomously operate in and modify unstructured environments would be extremely useful in a variety of applications, such as search and rescue and exploration of remote environments which lack the supply infrastructure required by typical construction techniques. Ideally, robots could modify their environment in ways that aid their immediate operational goals, or complete human imposed missions while requiring minimal or no additional raw materials.

Dry stacking, a construction technique that relies on gravity and friction instead of fasteners or mortar, is ideally suited for these applications. Rigid elements that are found in the environment are assembled into stable structures. Building these structures has long been the purview of expert human masons, and recent work by the authors [1], [2] and others [3] have investigated the feasibility of automating dry stacking as a robotic construction technique. In contrast to packing problems, in which objects need to be arranged into a fixed space, stacking problems are significantly more complicated due to additional stability constraints. Arrangements that achieve excellent packing can fail to be stable. Evaluating stability of structures is one of the key, necessary capabilities for automation.

One common approach to evaluate the stability of object arrangements is to subject them to disturbances such as loading forces and shaking. This method is common in both destructive physical testing and in a simulation. For simulated rigid bodies shaking (as opposed to loading) is especially appropriate, since the simulators fail to capture fractures and other compressive failures of individual elements accurately. However, simulated shaking is noisy, i.e. the same structure produces different results due to numerical noise and the choice of random forces and it is computationally expensive.

Analytic methods of modeling and analyzing stability have been widely used, e.g. in humanoid locomotion [4], [5], safety assessment of historic masonry structures [6], designing structural sound masonry building [7]. These methods provide analytic results or have computationally efficient implementations. However, these methods assume that the contact geometry is known or, in the case of design, can be efficiently parameterized. When working with found objects, robotic agents have limited choice of their exact shape and, therefore, have limited control over contact geometry, which makes it difficult to apply these analysis techniques directly.

In this paper, we study the stability evaluation for drystacked structures based on a geometric safety factor called *kern* [7]. When evaluating the stability of objects with plane-plane contacts, the kerning is applied to the interior portion of the contact interface, and stability can be evaluated by computing how much this interface can shrink and the overall structure still be stable. For example, in the case of vertical box stacking, the center of mass of the top objects needs to project onto the interior of this interface to be stable, so that smaller interfaces are less likely to be stable. The amount of possible shrinkage is a quantitative measure of stability. By expressing the torque and force balance between objects as a linear program, static stability can be checked quickly using a variety of commercial or free solvers. Our contribution is to formulate an approximation for the kern contact geometry that can be used on irregular objects. This enables a fast approximate stability analysis that can be used instead of shaking or a full simulation. This approach works particularly well for moderately irregular objects. Due to the increased speed, this novel methods can be used during the dry stacking assembly process and provide better results than the current, state-of-the-art techniques.

Section II gives a brief overview of related works; Section III describes the background knowledge and proposed algorithm; Section IV describes our specific simulation and experimental setup, results and subsequent discussion; finally Section V concludes the paper.

II. Related Work

In our previous work [1], [2], we propose an architecture for solving the dry stacking problem based on heuristics and deep Q-learning for building stable large-scale structures using physics simulation. The target structure is built on a simulated shaking table, and after a particular construction

[1]Authors are with Department of Computer Science and Engineering, University at Buffalo, Buffalo, NY 14260, USA yifangli,mairasab,vsangara,nnapp @buffalo.edu

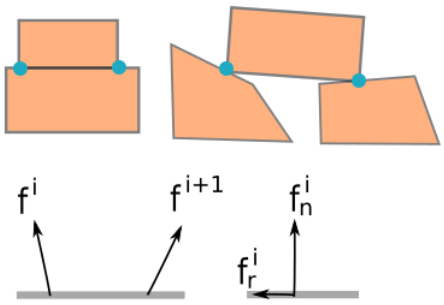

Fig. 1: Model of contact forces at interfaces between objects in 2D case. We assume there are two contact modes: point contact (point to line) in the upper right image and full contact (line to line) in the upper left one. A full contact can be represented as two-point contacts. Contact points are marked as blue color. At each contact, there is a force f^i, which can be decomposed into a normal force f_n^i and a friction f_r^i.

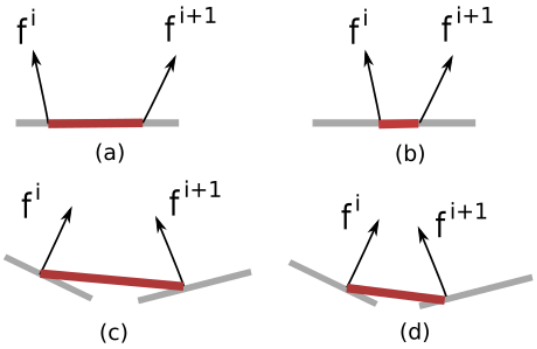

Fig. 2: Boundary shrinkage in 2D case. In (a), the original contacts are line to line contact, and red line represents kern. Two forces f^i and f^{i+1} are exerting to this kern; (b) shows the kern after several steps of shrinkage, and the forces f^i and f^{i+1} are closer. (c) gives example of point to line contact case, and after shrinkage, the forces are represented in (d). Force exerting locations are shrunk in a way that two forces are getting closer to each other along the direction of frictions.

experiment is completed, the whole structure is shaken and displacements of the objects are observed.

The methods presented by Furrer et al. [3] propose a pose searching algorithm that considers structural stability using a physics simulator. In addition, they present an autonomous system, using a robot manipulator, for stacking balancing vertical towers using irregular stones. Instead of analyzing contact forces directly, the pose searching method considers support polygon area, kinetic energy, the deviation between thrust line direction and the normal of the support polygon surface, and the length between the new object and the CoM of the previously stacked object.

Stability in assembly planning have been studied previously. Authors [8] addressed the problem of gravitational stability of assemblies of frictionless rigid bodies, and they proposed solution methods to the problems of determining if an assembly is stable and finding a stable orientation for a given assembly. Mosemann el al. [9] proposed methods to determine whether an assembly in a given orientation is frictional stable and to compute a frictional stable orientation.

Analyzing the stability of existing buildings using contact forces can serve as a useful tool in masonry. For example, structure stability analysis is used by Michiels et al. [10] to determine the collapse load and the collapse mechanism of a rammed earth arch; by Block et al. [6] for safety assessment of historic structures and by Panozzo et al. [11] to allow non-expert users to design masonry structures. Whiting et al. [7], proposed a measure of infeasibility that determines how close a model is to be structurally sound. Frick et al. [12] proposed methods that decompose three-dimensional shapes into self-supporting, discrete-element assemblies. Force networks in granular packing and force distributions are studied by Tighe et al. in [13] and Radjai at al. in [14]; and Groth et al. [15] investigate the acquisition of an intuitive understanding of physical principles and geometric affordances in the context of generalized object stacking.

Other applications also benefit from contact and force analysis. Caron et al. [4] proposed a closed form formula of the contact wrench cone [16] for rectangular support areas in rigid contacts situation. Addi and Rodic [5] investigated the impact and friction contact dynamics that occur during a biped motion. Zhou et al. [17] modeled 3D contact forces occurring during peg-in-hole assembly operations, in which the output force/torque is used for collision detection in an interactive virtual reality environment, as it affects the feedback perception.

III. Methods

In this section, we present the methods used for solving the static equilibrium equations and our proposed measure that uses the concept of kern. The notation is based on the approach in [7], which presents a more detailed derivation.

A. Static Equilibrium Analysis

A feasible structure is one in which the forces must satisfy static equilibrium, compression and friction constraints.

1) Contact Modeling: In 3D, the physics of contact is a continuous distribution of stress and pressure fields and surface contacts are often modeled using sets of contact points [18]. Authors in [18] prove that the distribution of contact forces on a plane is equivalent to contact forces lying in friction cones at the corners of convex contact polygons. Fig. 1 illustrates the contact forces discretization in 2D case.

2) Static Equilibrium: Static equilibrium conditions require that the net force and net torque, i.e the sum of all forces and torque, acting on objects in the structure equal zero, taking into account both gravity and external loads. We can combine the equilibrium constraints for each object into a linear system of equations [19] given by:

$$\mathbf{A}_{eq}.\mathbf{f} + \mathbf{w} = \mathbf{0} \tag{1}$$

where $\mathbf{w}$ is a vector containing the weights of each object, $\mathbf{f}$ is the vector of interface forces and $\mathbf{A}_{eq}$ is the matrix of coefficients for the equilibrium equations, see [7].

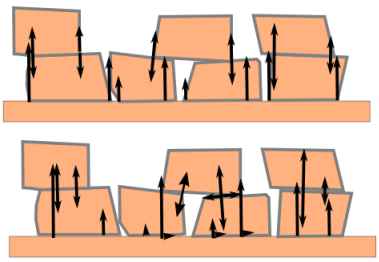

Fig. 3: Illustration of an example of boundary shrinkage. Top shows one set of feasible solution given original contacts; bottom is one feasible force solution after a few steps of shrinkage. Black arrow indicates the force magnitude and orientation.

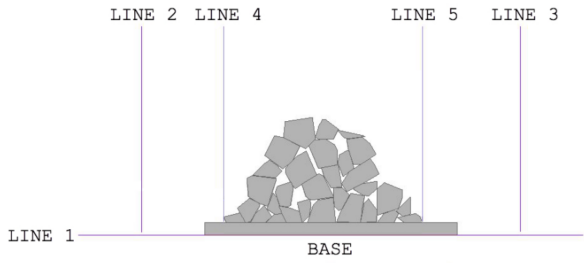

Fig. 4: Simulation framework. LINE 1 serves as the ground for the wall; LINE 2 and LINE 3 stop fallen objects from the wall from falling off screen; LINE 4 and LINE 5 are guidelines for the wall, and they do not interact with the environment; BASE at the bottom serves as the base for the wall construction.

3) Compression and Friction: Masonry uses building materials that are rigid. Hence, the compressive stresses are relatively low relative to the strength of masonry in such structures. Furthermore, according to limit analysis of masonry as summarized by [20], the material can be assumed to have zero tensile strength. This condition is expressed as a non-negativity constraint on the normal forces:

$$f_n^i \geq 0, \ \forall i \ \in \ \text{interface vertices} \tag{2}$$

In order to model friction, a friction constraint is applied to each vertex of the object interfaces. In Fig.1, for each pair of forces f_n^i and f_r^i, f_r^i lies within the friction cone of the normal force f_n^i. The linear approximation as a friction pyramid is given by :

$$|f_r^i| \leq \alpha f_n^i, \ \forall i \ \in \ \text{interface vertices} \tag{3}$$

where α is the coefficient of static friction; in this paper we use a value of 0.4. Combining the friction constraints for each object in the structure gives rise to a sparse linear system of inequalities:

$$\mathbf{A}_{fr}\mathbf{f} \leq 0 \tag{4}$$

In summary, for a feasible structure, a force solution must exist that satisfies the following linear constraints:

$$\begin{aligned} \mathbf{A}_{eq}.\mathbf{f} &= -\mathbf{w} \\ \mathbf{A}_{fr}.\mathbf{f} &\leq 0 \\ f_n^i \geq 0, \ \forall i \ &\in \ \text{interface vertices} \end{aligned} \tag{5}$$

Static analysis can only indicate whether a structure is stable or not. It fails to quantify stability, which allows for comparison of relative stabilities of different configurations for the same target structure. In addition, from a structural mechanics viewpoint, the constraints in Eq. 5 describe a statically indeterminate structure. Structures that have more unknown forces than available equilibrium equations are statically indeterminate [21], as the equations of local force and torque balance do not uniquely determine the forces.

B. Proposed Measure

Instead of solving for each individual force in response to various disturbances to quantify stability, we make use of the concept of *kern* [7] and check for global stability using the method described in the previous section. The kern is the central portion contact interface, possibly with additional safety margins, and the force equations are computed on the kern limits. If the resultant force lies within the kern boundaries, the entire interface will act in compression. If the resultant force reaches the boundary of the interface, the structure forms a hinge and might lead to unstable conditions. For example, in vertical box stacking or overhang problem, the resultant force of the top blocks needs to project inside the contact interface to be stable.

In our method, we systematically modify the kern limits by shrinking its boundaries. As the boundaries shrink, the corresponding force positions change and the static analysis equations are measured on the new positions. This procedure is repeated until there is no feasible solution for the static analysis equations. We associate the number of times that the kern can shrink and still allow for stable solutions as a measure of stability. Fig. 2 illustrates the boundary shrinkage in 2D case.

Algorithm 1 describes the proposed approach. In Line 3, the kern boundaries are shrunk by ϵ. At each shrinkage step, the locations of two forces move along their friction directions (Line 5). In line 6, we use COIN Cbc linear programming solver [22]. The return value of Algorithm 1 is how many times the interface can be shrunk, until the structure becomes infeasible. Fig. 3 illustrates an example of the boundaries shrinkage in our simulated environment. The proposed boundary shrinking method does not aim to calculate the exact force magnitude, and thus may not be able to accurately predict if an object is close to slipping. However, many real-world drystacked stone walls (Fig. 5 left) are constructed in such way that each stone is mostly supported by normal forces. In these situations friction forces seem to have limited contribution to the overall stability, and the proposed approximate method can yield good predictions.

IV. Experiments

We first describe the simulation environment used in our experiments, then we give the experimental results and further discussion. The objective of our experiment is to validate the proposed stability analysis, to compare its efficiency to the shaking analysis approach used in our

Data: Contacts, weight of each object
Result: shrinkage level
shrinkage level ← 0 ;
while *static analysis equations are feasible* **do**
    shrinkage level ← shrinkage level + 1 ;
    Shrink kern boundaries by ϵ ;
    Compute the new force positions;
    Apply linear programming solver on Eq. (5);
end

Algorithm 1: Kern based stability measure

Fig. 5: Real drystacked stone walls from masonry book [23].

previous experiments, and to test how much it can improve the heuristics-based planning if it is added to the assembly process. We conduct all the experiments using a Intel(R) Core(TM) i7-4790 CPU with 3.60GHZ computer.

A. Simulation

We developed our assembly framework based on a 2D rigid body simulator [24] that is necessary to provide the contact geometry used to predict the stability of structures. Fig. 4 depicts a screen shot of our framework.

In our previous work [1], [2], the structure stability is analyzed by shaking the platform (BASE) where the construction process takes place. During evaluation, the magnitude of shaking increases and the displacement of each object, as defined in Eq. (6), is measured. We define the parameterized lemniscate (∞-shaped) motions with different scaling factors as the shaking function. Let (x_t, y_t) be the coordinates of the BASE at time t, x_t and y_t move following $x_t = scale \times \cos(t)$ and $y = 0.5 \times scale \times \sin(2t)$ and $scale = shakeLevel/(3 - \cos(2t))$. Here, $scale$ indicates the magnitude of shaking; $shakeLevel$ denotes the scaling factor for the shaking function. Larger $shakeLevel$ generates larger velocity and magnitude for the BASE. After shaking, the displacement of each object is used to calculate the $stability$. The $shakeLevel$ keeps increasing until the built structure collapses, and this $shakeLevel$ is the final stability of current structure. The better quality a structure has, the more number of shaking levels it can withstand.

We calculate a displacement score D_{o_i} for each object o_i in the structure by taking into account its linear and angular displacement before and after the shaking process as shown below:

$$D_{o_i} = \sqrt{(\alpha \Delta x^2 + \alpha \Delta y^2 + \beta \Delta \theta^2)} \quad (6)$$

where Δx, Δy and $\Delta \theta$ are the differences in the horizontal direction, vertical direction and orientation of the object pose before and after the shaking process, respectively; α and β are scaling factors.

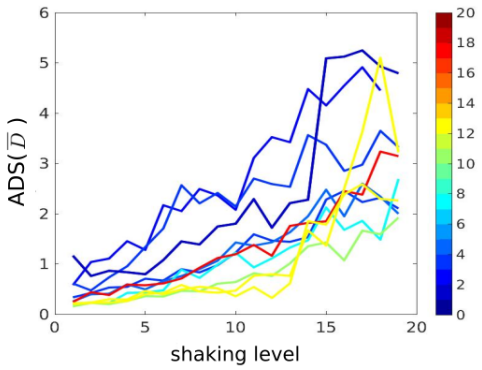

Fig. 6: Comparison between shaking test and proposed stability measure. Each colored continuous line represents one structure; horizontal axis is the shaking level; vertical axis represents the average displacement score of all objects after shaking test; and the colorscale shows the result of the proposed stability measure. Each color corresponds to one value on the color bar. Larger value on the color bar corresponds to larger stability value given by the proposed measure.

TABLE I: Comparison of running time. "Shaking evaluation" means after the target structure is completed, we test final structure by subjecting it to the shaking test, in which $shakingLevel$ increases from 1 to 20.

Method	Shaking (single)	Shaking evaluation	Proposed
Time (second)	5 to 10	150	<0.6

The Average Displacement Score (ADS) $\overline{D}$ is given by:

$$\overline{D} = \frac{1}{|I|} \Sigma_{o_i \in I} \; D_{o_i} \quad (7)$$

where I and $|I|$ represent the set and number of objects in the structure, respectively.

The shaking process is not an efficient way of evaluating stability. First, the simulation of the shaking is slow. Second, the process is non-deterministic due to numerical noise and the choice of random forces. For these reasons, in order to get reasonable stability value, shaking test needs to be conducted several times, which makes the evaluation more time-consuming.

B. Validation

Since a shaking test is one of the general ways of evaluating structure stability, we validate the proposed stability measure by comparing it to a shaking test.

TABLE I compares the running time between two measures. Single shaking test takes around 5 to 10 seconds, and this is 10 times slower than proposed measure. Once the structure is completed, a set of shaking test is conducted, where $shakingLevel$ increases from 1 to 20. This process usually takes around 150 seconds, which is 250 times slower than proposed measure.

In order to evaluate the proposed measure with less bias introduced by the existing stacking planning, we manually build different structures, which have different target area completions and level of stabilities. Fig. 6 shows the comparison between the shaking test and proposed measure. The

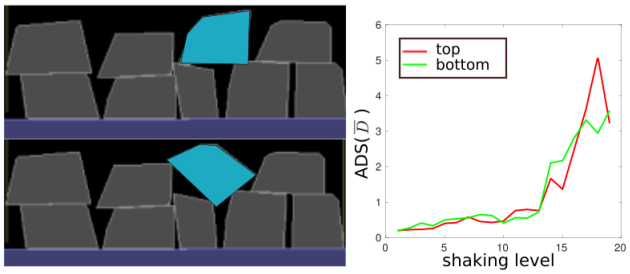

Fig. 7: An example in which the proposed measure outperforms the shaking test. Right image shows that the shaking test can not distinguish the top and bottom images on left in terms of stability, however, the proposed measure scores 13 to top left image, and 5 to bottom left one.

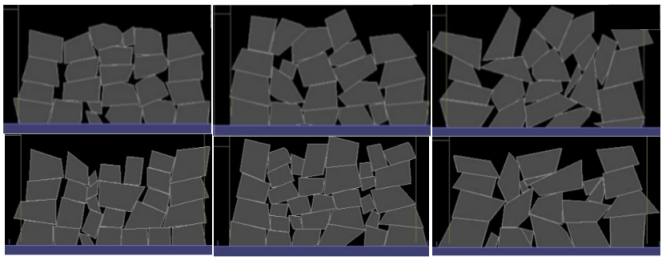

Fig. 8: Comparison between heuristics-based planning (top row) and combined planning (bottom row). From left to right, objects irregularity level is increasing.

colorscale shows the result of the proposed stability measure. The structures with lower stability measure are represented by blue lines, and they have larger ADS ($\overline{D}$) values; higher stability structures represented by yellow and red lines have lower ADS ($\overline{D}$) values. The proposed method correlates with the shaking method. Less stable structures produce more displacement for the same amount of shaking. From Fig. 6, we can see shaking test and proposed measure are complying with each other for most of the structures.

Fig. 7 illustrates an example of how a configuration difference in the positioning of a single object (the blue object) can affect the stability assessment provided by both methods. While the shaking test produces very similar results (green and red curves) for the given structures, the proposed measure generates more discrepant values (5 for the lower one and 13 for the upper one), as shown in the right image. In general, we would prefer the placement shown in the upper left image because the blue object in the lower left has the potential to push away other objects. While the proposed method can analytically identify it as a more stable configuration; the shaking test can not explicitly show that the upper is better than the lower.

C. Incorporating Heuristics

In previous work [1], we utilize the physics simulator to get a set of feasible poses for objects on a partially built structure. All the feasible poses respect both geometric and physical constraints. We then utilize heuristics for a reduction of the feasible poses set. The reduction is a hierarchical filtering approach, where each level filters out poses that do not meet the minimum requirement for a satisfactory placement. Each level of reduction uses heuristics derived from masonry books [25], [26]: the length of the common edges between objects, the hole area generated by a new placement, the height of neighboring objects, the top surface slope of an object after placement and if there is interlocking, see [1] for further explanations. Because the shaking process is computationally expensive, we only evaluate the stability of the structure after completion of the construction process.

Since the proposed stability measure takes less than 0.6 seconds to evaluate one structure, it can be added to previous heuristics-based planning as an additional level on the hierarchical filtering in each assembly step, which filters out poses whose shrinkage levels are less than the average number of shrinkage. This filter does not apply on small objects (fillers), see [1] for more details.

We evaluate the combined planning using datasets of irregular objects, as proposed in [1], in which the objects are categorized according to their levels of irregularity. In this work, we use objects whose irregularity levels range from 10 to 50, with a sampling interval of 10. For each irregularity level, we generated 5 different datasets and built 5 structures. The overall quality of the built structure is evaluated by:

$$Q = stability \times f(\text{TFF}) \tag{8}$$

where $stability$ is the $shakeLevel$, $f(\text{TFF})$ is a penalty function, where TFF stands for Target Fill Fraction. It is defined as the ratio of the area of the target structure that is not covered by the empty space to the area of target structure. The penalty function $f(\text{TFF})$ is defined as follows:

$$f(\text{TFF}) = \begin{cases} 0 & \text{TFF} < 60\% \\ \frac{1}{1+\exp\left(-a*(\text{TFF}-b)\right)} & \text{TFF} \geq 60\% \end{cases}$$

Fig. 9 depicts the overall quality of the previous heuristics-based greedy planning [1] and the combined planning described above. The black and red error bars are mean and standard deviation of the previous heuristics-based planning and the combined planning, respectively; the blue area is the prediction of heuristics-based planning given by Gaussian Process model with its probabilistic nature in the form of a pointwise $\pm\sigma$ confidence interval. Horizontal axis represents object dataset irregularity; a larger number corresponds to larger irregularities. The vertical axis is the overall quality of a structure.

For low levels of irregularity, the overall stability of combined planning outperforms the heuristics-based planning, but for higher irregularity, the results are similar in both methods, as we can see in Fig. 9. This is because more irregular objects have more complicated geometry, which is susceptible to contact geometry changes. So when the contact geometry changes, the prediction of stability based on previous contacts becomes invalid, which explains that when the level of irregularity increases, the combined method performs similar to the heuristics-based method.

Fig. 8 shows structures constructed using heuristics-based planning and combined planning. We can see that structures

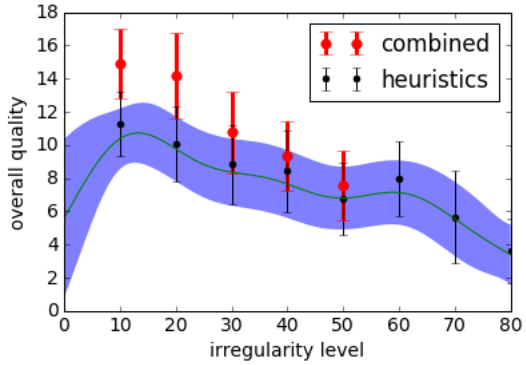

Fig. 9: Overall quality of assembly using object sets with different irregularities.

in the second row tend to have longer and more stable interfaces between objects than the ones in the first row. The structures in the last column are constructed with the dataset of objects that have high irregularity. This corresponds to Fig. 9 which, when the irregularity level is increasing, combined and heuristics-based planning performs similarly.

V. Conclusion

We study stability evaluation of drystacked structures. Using a full structural simulation subjected to disturbances is computationally expensive, and prohibitive when searching the space of possible assemblies. An approximate stability analysis is proposed based on *kern*. This method is known to be fast and accurate in regular contact geometries. Stability is estimated by shrinking the kern area until the structure becomes infeasible. This condition can be expressed as a linear program, where feasibility can be computed efficiently. However, with irregular objects, changes to the contact geometry are more difficult to compute and we propose a fast approximate approach to do so. Experiments verify that the resulting stability measure matches the evaluation of a fully simulated destructive shaking test. Due to the increased speed, this method can be added to existing heuristics-based planning during the assembly process. Experiments show that the combined assembly planning outperforms the heuristics-based method, especially for dry-stacking moderately irregular objects where the contact change approximation is good.

Acknowledgements

We are also grateful for the Science Without Borders Program (CAPES #013584/2013-08), NSF Grant #1846340 and the Computer Science and Engineering Department at the University at Buffalo for supporting this work.

References

[1] V. Thangavelu, Y. Liu, M. Saboia, and N. Napp, "Dry stacking for automated construction with irregular objects," in *2018 IEEE International Conference on Robotics and Automation (ICRA)*. IEEE, 2018, pp. 1–9.

[2] Y. Liu, S. M. Shamsi, L. Fang, C. Chen, and N. Napp, "Deep q-learning for dry stacking irregular objects," in *2018 IEEE/RSJ International Conference on Intelligent Robots and Systems (IROS)*. IEEE, 2018, pp. 1569–1576.

[3] F. Furrer, M. Wermelinger, H. Yoshida, F. Gramazio, M. Kohler, R. Siegwart, and M. Hutter, "Autonomous robotic stone stacking with online next best object target pose planning," in *Robotics and Automation (ICRA), 2017 IEEE International Conference on*. IEEE, 2017, pp. 2350–2356.

[4] S. Caron, Q.-C. Pham, and Y. Nakamura, "Stability of surface contacts for humanoid robots: Closed-form formulae of the contact wrench cone for rectangular support areas," in *Robotics and Automation (ICRA), 2015 IEEE International Conference on*. IEEE, 2015, pp. 5107–5112.

[5] K. Addi and A. Rodić, "Impact dynamics in biped locomotion analysis: Two modelling and implementation approaches," *AIMS Journal on Mathematical Biosciences and Engineering*, vol. 7, no. 3, pp. 479–504, 2010.

[6] P. P. C. V. Block, "Thrust network analysis: exploring three-dimensional equilibrium," Ph.D. dissertation, Massachusetts Institute of Technology, 2009.

[7] E. Whiting, J. Ochsendorf, and F. Durand, "Procedural modeling of structurally-sound masonry buildings," in *ACM Transactions on Graphics (TOG)*, vol. 28, no. 5. ACM, 2009, p. 112.

[8] R. Mattikalli, P. K. Khosla, B. Repetto, and D. Baraff, "Stability of assemblies," in *Intelligent Robots and Systems' 93, IROS'93. Proceedings of the 1993 IEEE/RSJ International Conference on*, vol. 1. IEEE, 1993, pp. 652–661.

[9] H. Mosemann, F. Rohrdanz, and F. M. Wahl, "Stability analysis of assemblies considering friction," *IEEE Transactions on Robotics and Automation*, vol. 13, no. 6, pp. 805–813, 1997.

[10] T. Michiels, R. Napolitano, S. Adriaenssens, and B. Glisic, "Comparison of thrust line analysis, limit state analysis and distinct element modeling to predict the collapse load and collapse mechanism of a rammed earth arch," *Engineering Structures*, vol. 148, pp. 145–156, 2017.

[11] D. Panozzo, P. Block, and O. Sorkine-Hornung, "Designing unreinforced masonry models," *ACM Transactions on Graphics - SIGGRAPH 2013*, vol. 32, no. 4, pp. 91:1–91:12, July 2013.

[12] U. Frick, T. Van Mele, and P. Block, "Decomposing three-dimensional shapes into self-supporting, discrete-element assemblies," in *Modelling Behaviour*. Springer, 2015, pp. 187–201.

[13] B. P. Tighe, J. H. Snoeijer, T. J. Vlugt, and M. van Hecke, "The force network ensemble for granular packings," *Soft Matter*, vol. 6, no. 13, pp. 2908–2917, 2010.

[14] F. Radjai, S. Roux, and J. J. Moreau, "Contact forces in a granular packing," *Chaos: An Interdisciplinary Journal of Nonlinear Science*, vol. 9, no. 3, pp. 544–550, 1999.

[15] O. Groth, F. Fuchs, I. Posner, and A. Vedaldi, "Shapestacks: Learning vision-based physical intuition for generalised object stacking," *arXiv preprint arXiv:1804.08018*, 2018.

[16] D. J. Balkcom and J. C. Trinkle, "Computing wrench cones for planar rigid body contact tasks," *The International Journal of Robotics Research*, vol. 21, no. 12, pp. 1053–1066, 2002.

[17] J. Zhou, N. D. Georganas, E. M. Petriu, X. Shen, and F. Marlic, "Modelling contact forces for 3d interactive peg-in-hole virtual reality operations," in *Instrumentation and Measurement Technology Conference Proceedings, 2008. IMTC 2008. IEEE*. IEEE, 2008, pp. 1397–1402.

[18] S. Caron, "Computational foundation for planner-in-the-loop multi-contact whole-body control of humanoid robots," Ph.D. dissertation, University of Tokyo, 2016.

[19] R. K. Livesley, "Limit analysis of structures formed from rigid blocks," *International Journal for Numerical Methods in Engineering*, vol. 12, no. 12, pp. 1853–1871, 1978.

[20] J. Heyman, *The stone skeleton: structural engineering of masonry architecture*. Cambridge University Press, 1997.

[21] R. C. Hibbeler and T. Kiang, *Structural analysis*. Prentice Hall, 1984, vol. 9.

[22] R. Lougee-Heimer, "The common optimization interface for operations research: Promoting open-source software in the operations research community," *IBM Journal of Research and Development*, vol. 47, no. 1, pp. 57–66, 2003.

[23] M. Cook, *Stone Walls*. Damiani Editore, 2011.

[24] Pybox2d. [Online]. Available: https://github.com/pybox2d/pybox2d

[25] J. Vivian, *Building Stone Walls*. Storey Publishing, 1976.

[26] C. McRaven, *Building stone walls*. Storey Publishing, 1999, vol. 217.